HHS Public Access

Author manuscript

Glia. Author manuscript; available in PMC 2015 May 28.

Published in final edited form as:

Glia. 2013 November ; 61(11): 1906–1921. doi:10.1002/glia.22567.

Cdc42 Regulates Schwann Cell Radial Sorting and Myelin Sheath Folding Through NF2/Merlin-Dependent and Independent Signaling

Li Guo, **Chandra Moon**, **Yi Zheng**, and **Nancy Ratner**

Division of Experimental Hematology and Cancer Biology, Department of Pediatrics, Cincinnati Children's Hospital, University of Cincinnati, Cincinnati, Ohio

Abstract

The Rho family GTPase Cdc42 has been implicated in developmental Schwann cell (SC) proliferation, providing sufficient SCs for radial sorting of axons preceding SC differentiation in the peripheral nervous system. We generated Cdc42 conditional knockout (Cdc42-CKO) mice and confirmed aberrant axon sorting in Cdc42-CKO nerves. In adult Cdc42-CKO nerves, blood vessels were enlarged, and mature Remak bundles containing small axons were absent. Abnormal infoldings and outfoldings of myelin sheaths developed in Cdc42-CKO nerves, mimicking pathological features of Charcot-Marie-Tooth (CMT) disease. The NF2/merlin tumor suppressor has been implicated up- and down-stream of Cdc42. In Cdc42-CKO;NF2-del double mutant mice, radial sorting defects seen in Cdc42-CKO nerves were rescued, while changes in myelin sheaths in Cdc42-CKO nerves were not. Phosphorylation of Focal adhesion kinase (FAK) and P-GSK3β, as well as expression of β-catenin were decreased in Cdc42-CKO nerves, and these changes were rescued by NF2/merlin mutation in Cdc42-CKO;NF2-del double mutant mice. Thus, Cdc42 regulates SC radial sorting *in vivo* through NF2/merlin dependent signaling pathways, while Cdc42 modulation of myelin sheath folding is NF2/merlin independent.

Keywords

rho; charcot-marie-tooth; collagen; catenin; FAK

Introduction

Schwann cell (SC) proliferation and differentiation are precisely regulated in developing peripheral nerves. Embryonic SCs originate from migrating neural crest cells and, while proliferating, differentiate into SC precursors, then differentiate into immature SCs (Jessen and Mirsky, 2005). Differentiation of the immature SC into mature SC occurs around birth via a process called radial sorting. During radial sorting SCs extend processes into axon bundles and segregate axons (Chernousov et al., 2008; Martin and Webster, 1973; Webster

Address correspondence to Nancy Ratner, 3333 Burnet Ave., ML 7013, CCHMC, Cincinnati, OH 45229, USA., Nancy.Ratner@cchmc.org.

Additional Supporting Information may be found in the online version of this article.

et al., 1973). SCs associated with a single large diameter axon will develop into myelinating SCs, while nonmyelinating SCs persistently ensheath multiple small diameter axons into Remak bundles (Jessen and Mirsky, 2005). A laminin-rich basal lamina surrounds all SCs, and SC laminins are required for SC morphogenesis.

Rho family GTPase proteins are molecular switches. These GTPases cycle between a GTP-bound active form, in which they signal to downstream effector proteins, and a GDP-bound inactive form (Bos et al., 2007). Guanine exchange factors (GEFs) enhance GTP-loading of GTPases, while guanine activating proteins (GAPs) accelerate GTP hydrolysis, thereby inactivating GTPases. Previous *in vitro* studies implicated the small Rho family GTPase Cdc42 in neurotrophin regulated SC migration (Yamauchi et al. 2005). *In vivo* studies implicated Cdc42 in perinatal SC proliferation, allowing for proper radial sorting (Benninger et al., 2007; Nodari et al., 2007). In addition, axon sorting deficits in SC lacking laminins were improved after forced activation of Cdc42 and/or the related small GTPase Rac1 (Yu et al., 2009).

The importance of Rho family GTPases in SCs has been highlighted by recent findings that mutations in FRABIN, a Cdc42 specific GEF, cause peripheral nerve demyelination and abnormal myelin infoldings and outfoldings in patients with autosomal recessive Charcot-Marie-Tooth (CMT) neuropathy (Delague et al., 2007; Fabrizi et al., 2009; Stendel et al., 2007). A cell autonomous role for Frabin in SCs was established in mice lacking Frabin, which recapitulated the human myelin phenotypes and showed decreased Cdc42-GTP (Horn et al., 2012). Mutations in the Cdc42 interacting protein INF2 also cause CMT disease (Boyer et al., 2011). While the CMT neuropathies together occur in 1:2,500 persons, making them a common cause of peripheral nerve dysfunction, the downstream effectors of Cdc42 in SC differentiation and peripheral neuropathies remain unknown.

One protein implicated both upstream and downstream of Cdc42 signaling is NF2/merlin, the protein product of the *neurofibromatosis type* 2 (NF2) gene. Supporting a role for NF2/merlin in peripheral nerve, NF2 mutation predisposes affected patients to SC tumors (Evans et al., 1992). NF2/merlin negatively regulates Cdc42 activity. For example, Cdc42-GTP is increased in human *Nf2* mutant schwannoma cells and $Nf2^{-/-}$ fibroblasts, and NF2/merlin mutant schwannoma cells show multiple filopodia characteristic of elevated active Cdc42-GTP (Flaiz et al., 2007; Thaxton et al., 2007; Xiao et al., 2002). NF2/merlin is an ezrin-radixin-moesin (ERM) family protein regulated by conformational change. A previous study suggests that Cdc42 regulates NF2/merlin phosphorylation on serine 518 via p21-activated kinase (PAK), a common downstream target of Cdc42 (Xiao et al., 2002). PAK mediated phosphorylation alters NF2/merlin conformation and interaction with binding partners (Rong et al., 2004; Ye, 2007). Interestingly, laminins can stimulate phosphorylation of the NF2/merlin in cultured SC (Thaxton et al., 2008). In cultured SCs lacking laminin, merlin phosphorylation and Cdc42 activity is decreased (Yu et al., 2009). Thus, we hypothesized that a feedback loop between Cdc42 and NF2/merlin may be critical for Cdc42 function in SCs.

To analyze the *in vivo* role of NF2/merlin in Cdc42-regulated radial sorting in SCs, we generated Cdc42-CKO;NF2-del double mutant mice by breeding Cdc42-CKO mice (in

which Cdc42 was conditionally ablated in SCs) and NF2-del mice (transgenic mice that express dominant negative NF2 mutant protein in SCs) (Giovannini et al., 1999). Our data show that Cdc42 regulates SC radial sorting *in vivo* through NF2/merlin, while Cdc42 modulates myelin sheath folding in a NF2/merlin independent manner.

Materials and Methods

Generation of DhhCre Directed Conditional Cdc42 Knockout Mice

Cdc42$^{flox/flox}$ mice were bred to Dhh-Cre mice (Jaegle et al., 2003) to obtain *Dhh-Cre1+; Cdc42*$^{flox/flox}$ (Cdc42-CKO) mice. Littermate *Dhh-Cre; Cdc42*$^{flox/WT}$ mice were used as controls. The genotype of *Dhh* and *Cdc42* alleles were analyzed by PCR as previously described. The primers for *Dhh* were sense: 5′-ACCCTGTTACGTATAGCCGA-3′ and anti-sense: 5′-CTCGGTATTAAACTCCAG-3′. The primers for Cdc42 were sense: 5′-TACAGTTGGTACATATTCCGATGGG-3′ and anti-sense: 5′-AGACAAAACAACAAGGTCCAGAAAC-3′. Primer 5′-CTGCCAACCATGACAACCTAAGTTC–3′ was used to identify the *Cdc42* knockout band. NF2-del mice are transgenic mice (*P0-SCH-*Δ*39–121*) expressing a mutant NF2/merlin, in which exons 2 and 3 (amino acids 39–121) are deleted from the genomic sequence, mimicking a human mutation (Giovannini et al., 1999). This NF2/merlin mutant allele is expressed under the control of a SC-specific P0 promoter. These mice were intercrossed with Cdc42 knockout mice to generate *DhhCre+;Cdc42*$^{flox/flox}$*;NF2-del* (Cdc42-CKO;NF2-del) mice. Littermate *Dhh-Cre−; Cdc42*$^{flox/WT}$*; NF2-wt* genotype mice were used as controls. Dhh-Cre mice were maintained on the C57BL/6 background. *Cdc42*$^{flox/flox}$ mice were maintained on a mixed 129Sv and C57BL/6J background. NF2-del mice were maintained on the FVB/N background. All animal experiments were conducted in mixed gender mice.

Electron Microscopy

Mice were anesthetized, then perfused and fixed with electron microscopy fixative (3% paraformaldehyde and 3% glutaraldehyde in phosphate buffered saline, pH 7.4–7.6). Sciatic nerves of wild type and mutant mice at ages designated in the text were dissected, post-fixed, osmicated, embedded and sectioned. High magnification pictures of ultrathin sections were taken on a Hitachi H-7600 transmission electron microscope following staining with lead citrate and uranyl acetate.

Western Blots

Sciatic nerve tissue was homogenized using a TissueRuptor (Qiagen) and lysed in lysis buffer (20 mM $NaPO_4$, 150 mM NaCl, 2 mM $MgCl_2$, 0.1% Nonidet P-40, 10% glycerol, 10 mM sodium fluoride, 0.1 mM sodium orthovanadate, 10 mM sodium pyrophosphate, 10 nM okadaic acid, 1 mM dithiothreitol, 10 μg mL^{-1} leupeptin, 10 μg mL^{-1} aprotinin, 10 μg mL^{-1} pepstatin, 10 μg ml^{-1} tosyl-L-phenylalanine chloromethyl ketone, and 10 μg mL^{-1} N-α-tosyl-L-lysine chloromethyl ketone). Homogenates were centrifuged at 10,000g for 10 min and protein extract supernatants were collected. Protein concentration was measured on a spectrophotometer using Bio-Rad DC Protein Assay Kit (Bio-Rad). Equal amounts of protein were fractionated by 4–20% SDS-PAGE and transferred to PVDF membranes.

Membranes were incubated with primary antibodies followed by appropriate secondary antibodies, and developed by Amersham ECL Detection Reagents (GE Healthcare Biosciences). The following primary antibodies from Cell Signaling were used: Cdc42 (1:500), P-merlin (1:500), merlin (1:800), P-PAK1/2 (1: 1000), PAK (1:1000), P-GSK3β (1:1000); GSK3β (1:1000); P-FAK (1:500); β-Catenin (1:1000); P-Erk (1:2000), and β-actin (1:10000). Active anti-β-Catenin (1:500) was purchased from Millipore. Anti-rabbit and anti-mouse HRP conjugated secondary antibodies (1:5000) were purchased from Bio-Rad.

Immunohistochemistry

Mice were anesthetized and perfused with 4% paraformaldehyde. Sciatic nerves were dissected and fixed in 4% paraformaldehyde (PFA) overnight. For cryostat sections, fixed sciatic nerves were incubated in 20% sucrose buffer and then frozen in OCT compound (Sakura). Frozen blocks were cut into 6–8 μm frozen sections using a Leica Cryostat. For paraffin sections, fixed sciatic nerves were incubated in 70% ethanol then processed in paraffin wax. Paraffin blocks were cut into 4 μm paraffin sections. Paraffin sections were deparaffinized and rehydrated before staining. Sodium citrate buffer (pH 6.0) was used for antigen unmasking. Sections were blocked for 1 h with blocking buffer (10% serum in PBS) and incubated with Ki67 primary antibody (Ventana) at 4°C overnight. The next day, the ABC avidin/biotin method was used to visualize Ki67 staining. Sections were counterstained with hematoxylin to visualize nuclei. Ki67-labeled cells and the counterstained total nuclei were counted to define percentages of proliferating cells.

BrdU Incorporation and Staining

Mice were injected with bromodeoxyuridine (BrdU, Sigma-Aldrich) (50 mg kg^{-1} of body weight) three times at 3-h intervals. Twenty-four hours after the first injection, mice were perfused with 4% paraformaldehyde; cryostat sections were stained with an anti-BrdU antibody (Abcam). Nuclei were stained with DAPI. BrdU-labeled cells and DAPI stained nuclei were counted to define percentages of proliferating cells.

Schwann Cell Culture

Sciatic nerves were sterilely dissected from euthanized P30 mice and incubated at 37°C, 7.5% CO_2 in DMEM medium (Invitrogen) supplemented with 10% fetal bovine serum (Gemini Bio-Products), 1% penicillin-streptomycin (Fisher Scientific), forskolin (2 μM, Calbiochem), and β-heregulin (HRG, 10 ng mL^{-1}, R; D Systems). This medium was replaced every 2 days. After 6–9 days nerves were incubated in dissociation medium [Leibovitz medium (Invitrogen) containing collagenase type I (130 U mL^{-1}, Worthington Biochemical Corporation, Lakewood, NJ), dispase II (2.5 mg mL^{-1}, Roche Diagnostics, Indianapolis, IN), gentamycin (50 μg mL^{-1}, Lonza walkersville), fungizone (2.5 μg mL^{-1}, Invitrogen)] for 3 h at 37°C. Cells were dissociated using a narrowed Pasteur pipette then were centrifuged for 5 min at 1000 rpm. Cells were resuspended in DMEM/F-12 medium (Invitrogen) supplemented with N2 supplement solution (Invitrogen), forskolin (2 μM, Calbiochem), β-heregulin (HRG) (10 ng mL^{-1}), gentamycin (50 μg mL^{-1}, Lonza) and fungizone (2.5 μg mL^{-1}, Invitrogen). Cells were plated on poly-L-lysine (Sigma) and laminin (BD Biosciences) coated plates and incubated at 37°C, 7.5% CO_2. Medium was

changed every 3 days and the cells were passaged when confluent. Cells were used at passages 0 or 1 and cell morphology monitored by light microscopy. For staining, cells were fixed and stained with phalloidin (Invitrogen) and an antibody recognizing the SC marker, P75NTR (Millipore).

Morphometric Quantification and Statistical Analysis

Morphometric measurements of axonal sorting and myelination were performed in electron microscopic images of sciatic nerve cross sections. A cell counter plugin from ImageJ software was used to analyze the number of one-to-one myelinated axons, nonmyelinated axons, and the axon number in each axonal bundle. Statistical significance was determined between two individual samples with the Student's *t* test. For multiple comparisions, one-way ANOVA followed by Tukey's post hoc test was used. Significance was denoted as $*P < 0.05$, $**P < 0.01$, or $***P < 0.001$.

Results

Conditional Knockout of Cdc42 in SCs in vivo

To analyze the role of the small GTPase Cdc42 in SCs *in vivo*, Cdc42 conditional knockout mice (Cdc42-CKO) were generated using the Cre recombinase (Cre)-LoxP recombination system under the control of *desert hedgehog* (Dhh) gene. In these mice, Dhh activates Cre recombinase expression in SCs at embryonic day (E) 12.5 (Jaegle et al., 2003; Wu et al., 2008). Exon2 of Cdc42 alleles were excised upon Dhh-Cre recombination (Fig. 1A). The Cdc42 knockout alleles were confirmed by PCR (Fig. 1B).

Conditional knockout of Cdc42 in SCs led to hind limb dysfunction with abnormal hindlimb clasping in mutant mice at postnatal day (P) 30 (Fig. 1C). The mice developed tremors but did not become paralyzed. Cdc42-CKO mice lived over 6 months provided food was easily accessible. At P30, sciatic nerves from Cdc42-CKO were thinner than sciatic nerves from wild type mice (Fig. 1D). Significant reduction of Cdc42 protein expression in mutant sciatic nerves was verified by western blot (Fig. 1E,F).

Abnormalities in Cdc42-CKO Sciatic Nerves

Sciatic nerves from adult Cdc42-CKO mice were compared to nerves from control mice. In semithin plastic sections evaluated at the light microscope level, we observed many large pale areas in Cdc42-CKO nerves (Fig. 2A, asterisks), identified as large bundles of unsorted axons in Cdc42-CKO nerves by electron microscopy (EM) (Fig. 2B, arrows). Although there were many myelin sheaths formed in the absence of Cdc42, myelin sheath structure was frequently abnormal (Fig. 2A, arrows; and see Fig. 4). We also observed that the size of the blood vessel was increased in Cdc42-CKO sciatic nerves (arrowheads in Fig. 2A,C). Enlarged blood vessels in nerves were also observed in the absence of N-WASP, a downstream effector of Cdc42 (Jin et al., 2011).

Nerve ultrastructure in Cdc42-CKO mice sciatic nerves was compared to control mice by electron microscopy (EM) at several ages. At P1, large unsorted axon bundles were observed in Cdc42-CKO sciatic nerves; in contrast, some axons had already been sorted and

were thinly myelinated in control sciatic nerves (Fig. 3A). At P30, P60 and P120, abnormally large axon bundles, containing unsorted large and small diameter axons, persisted in adult Cdc42-CKO sciatic nerves (Fig. 3A, asterisks). In contrast, large axons in control sciatic nerves were well myelinated and small axons were segregated by SCs and formed Remak bundles (Fig. 3A, arrows). The numbers of myelinated axons in adult nerves were similar in control and Cdc42-CKO sciatic nerves (Fig. 3B) while numbers of non-myelinated axons and axons/bundle were increased significantly at P30, P60 and P120 in Cdc42-CKO nerves (Fig. 3C,D). While normal mature Remak bundles contain small axons individually ensheathed by membrane-delimited SC cytoplasm processes (Fig. 3E, arrow), in Cdc42-CKO mice axons touched each other with no intervening SC processes (Fig. 3E, asterisk). At all ages, SC nuclei remained at the outside of unsorted axon bundles in Cdc42-CKO nerves, a phenotype normally present only in embryonic nerves (Jessen and Mirsky, 2005). Our observations indicate that Cdc42 is critical for axonal sorting, which necessitates extending processes into axon bundles. However, once sorted into 1:1 relationship with large axons, Cdc42-CKO SCs are able to myelinate axons.

Aberrant Myelin Morphology in Cdc42-CKO Sciatic Nerves

In addition to the profound failure of radial sorting, many myelin sheaths in sciatic nerves from Cdc42-CKO mice differed from those of wild type animals (Fig. 3A, arrowheads), and at low magnification semithin plastic sections often contained densely stained areas associated with myelin sheaths (Fig. 2A, white arrows). Electron microscopy of Cdc42-CKO sciatic nerves provided evidence of a dysmyelination phenotype caused by loss of Cdc42. Cdc42-CKO nerve fibers contained abnormal features including myelin infoldings and outfoldings with redundant myelin loops (Fig. 4A). These features were present in about 10% of myelinated fibers (Fig. 4B). Occasionally, myelin sheaths wrapped around unsorted axons (Fig. 4A, arrow). We also observed signs of axonal degeneration and regeneration in Cdc42-CKO nerves, with accumulation of axonal organelles in myelinated and unmyelinated fibers (Fig. 4C) and regenerating clusters of axons with thin myelin sheaths in Cdc42-CKO nerves (Fig. 4A, arrowhead). These results suggest that Cdc42 is required for maintenance of normal myelin sheaths.

Axonal Sorting Defects in Cdc42-CKO Mice are Rescued by NF2/Merlin Mutant

NF2/merlin is related to Cdc42 signaling in SCs (Thaxton et al., 2007; Xiao et al., 2002; Zhan and Chadee, 2010). Whether NF2/merlin is critical for Cdc42 function in SCs *in vivo* is unknown. To test if NF2/merlin function is critical for radial sorting defects and abnormal myelin sheath folding in Cdc42-CKO mice, Cdc42 knockout mice were intercrossed with NF2-del transgenic mice that express dominant negative NF2 mutant protein (Denisenko et al., 2008; Giovannini et al., 1999). We confirmed SC hyperplasia in NF2-del transgenic mouse nerves and found no sorting defects or myelin defects in nerve cross sections at P30 or P180 (not shown). Strikingly, sciatic nerves in Cdc42-CKO;NF2-del double mutant mice were restored to nearly the size of control sciatic nerves (Fig. 5A). While 2-month-old Cdc42-CKO sciatic nerves contained numerous bundles of unsegregated large and small axons without the SC ensheathment characteristic of mature Remak bundles, most axon bundles were sorted by SCs processes extending around individual axons in Cdc42-CKO;NF2-del double mutant sciatic nerves (Fig. 5B). At high magnification, it became clear

that Cdc42-CKO;NF2-del double mutant mice showed improved segregation with SC processes separating small axons, while axons touched each other with no intervening SC processes in Cdc42-CKO mice (Fig. 5C). Furthermore, while large axons were common in unsorted bundles in Cdc42-CKO nerves, in double mutants the axon bundles contained only small axons. Although axons became individually wrapped within axon bundles in Cdc42-CKO;NF2-del double mutant mice, these axon bundles were not normal Remak bundles; rather, individual axons were separately wrapped by SCs. Quantification showed a significant improvement in sorting of axons in Cdc42-CKO;NF2-del double mutant nerves compared to that in Cdc42-CKO nerves (Fig. 5D). These data suggest that Cdc42 normally promotes axonal sorting through NF2/merlin dependent signaling.

To determine whether unsorted axon bundles evolve into sorted bundles or whether axon sorting is rescued early in double mutants, we analyzed Cdc42-CKO and Cdc42-CKO;NF2-del double mutant nerves at P15. Large bundles of unmyelinated unsorted axons were present in CDC42-CKO nerves at P15; the unsorted bundles contained many large axons. In the Cdc42-CKO;NF2-del double mutants, bundles of unmyelinated axons contained mainly small axons, and larger axons were often present at the edges of bundles and some large fibers were thinly myelinated (Fig. 5E). Thus, NF2 mutation accelerates sorting in Cdc42-CKO mutants.

Proliferation in Cdc42-CKO and Cdc42-CKO;NF2-del Double Mutant Mice

It was suggested that Cdc42 effects on SC proliferation account for effects on radial sorting (Benninger et al. 2007). To test if the rescue of axonal sorting in Cdc42-CKO;NF2-del double mutant mice results from effects on cell proliferation, we measured SC proliferation by BrdU incorporation. We observed a significant increase of SC proliferation in P30 Cdc42-CKO and Cdc42-CKO;NF2-del double mutant nerves (Supp. Info. Fig. 1A,B). There was no significant difference in the percentage of BrdU-positive cells or total nuclei number when comparing Cdc42-CKO with Cdc42-CKO;NF2-del nerves (Supp. Info. Fig. 1C–E). We also measured SC proliferation at P0 and found no difference in the percentage of Ki67-positive cells in Cdc42-CKO nerves compared with control nerves (Supp. Info. Fig. 1F,G). These results suggest that the rescue of axonal sorting defects in Cdc42-CKO nerves by NF2/merlin mutation in Cdc42-CKO;NF2-del double mutant mice are not related to altered cell proliferation.

Aberrant Myelin Morphology in Cdc42-CKO Sciatic Nerves is Independent of NF2/Merlin

Myelin morphology was analyzed in Cdc42-CKO;NF2-del double mutant sciatic nerves by electron microscopy. The abnormal myelin structure characteristic of Cdc42-CKO nerves, including myelin infoldings and outfoldings, persisted in Cdc42-CKO;NF2-del double mutant sciatic nerves (Fig. 6A, arrows). Axon degeneration and myelin debris also persisted (Fig. 6B). These results suggest that Cdc42 function in myelin sheath organization is independent of NF2/merlin.

In addition, redundant SC process within axonal bundles (arrowheads), empty basal lamina loops (arrow), collagen pockets (asterisks) (which are collagen surrounded by SC processes), and SC processes without axon contact were frequently observed in Cdc42-

CKO;NF2-del double mutant nerves (Fig. 6C), suggesting that axonal sorting signals may be over-activated in the double mutant mice. We observed a few collagen pockets in NF2-del mice and none in Cdc42-CKO mice; Denisenko et al. (2008) also identified a few collagen pockets in NF2-del mice and P0Cre; $NF2^{flox2/flox2}$ mice. There were significantly more collagen fibers wrapped by SCs in Cdc42-CKO;NF2-del double mutant mice. One interpretation of this dramatic result is that Cdc42 acts downstream of NF2/merlin to suppress ectopic process formation.

Phosphorylation of PAK at Thr423(PAK1)/ Thr402(PAK2) and Phosphorylation of NF2/ Merlin at Ser518 are not Affected by Cdc42 Deletion

Phosphorylation of NF2/merlin can be regulated by PAK, a Cdc42 effector (Rong et al., 2004; Xiao et al., 2002; Ye, 2007). Thus, we predicted that NF2/merlin phosphorylation will decrease in the absence of Cdc42. We analyzed the phosphorylation (activation) of Pak and the phosphorylation of NF2/merlin in control and Cdc42-CKO sciatic nerves by western blotting. Surprisingly, phosphorylation of PAK at Thr423(PAK1)/ Thr402(PAK2) and phosphorylation of merlin at Ser518 remained unchanged in Cdc42-CKO sciatic nerves at P30 (Fig. 7A). The results suggest Cdc42 may regulate NF2/merlin function independent of such phosphorylation events.

Altered Phosphorylation of FAK and GSK3β/β-Catenin Signaling is Restored by Mutation of NF2/ Merlin

To study downstream molecules potentially affected by Cdc42-CKO and/or NF2/merlin mutation, nerve lysates from mutant mice were analyzed by western blotting. We searched for changes specific to loss of Cdc42, and rescued by NF2/merlin mutation. Phosphorylation of GSK3β and expression of β-catenin were significantly decreased in Cdc42-CKO nerves, and both were restored by mutation of NF2/merlin (Fig. 7B). In contrast, no changes in phosphorylation of ERK were detected in Cdc42-CKO nerves compared to wild-type nerves. Focal adhesion kinase (FAK) has been implicated in SC radial sorting (Grove et al., 2007). We observed phosphorylation of FAK was decreased in Cdc42-CKO nerves and was restored by mutation of NF2/merlin. Reduced P-FAK in cell lysates from cultured Cdc42-CKO SCs was also rescued by NF2/merlin mutation in cultured Cdc42-CKO;NF2-del double mutant SCs (Fig. 7C). Thus, phosphorylation of FAK and regulation of GSk3β/ β-catenin signaling are altered in Cdc42-CKO nerves, and expression is normalized in double mutants; future studies will be necessary to address whether these changes are causal in the phenotypes.

SC Morphology in vitro is Altered by Cdc42-CKO

Extensive evidence supports a role of Cdc42 in filopodia formation in many cell types, including SCs (Flaiz et al., 2007). Primary SCs were cultured from P30 sciatic nerves of control, Cdc42-CKO, NF2-del and Cdc42-CKO;NF2-del double mutant mice. Cdc42-CKO cultures showed significantly increased SC process numbers and increased numbers of lamellipodia, compared to control SCs (Fig. 8). In contrast, SC process length was not significantly affected by Cdc42 loss (Fig. 8E). Neither process number nor increased numbers of lamellipodia in Cdc42-CKO SCs were rescued by NF2/ merlin mutation in

Cdc42-CKO;NF2-del double mutant SCs (Fig. 8D,F). These results suggest that Cdc42 regulates SC process number and lamellopodia independent of NF2/merlin signaling.

Discussion

Our studies confirm the finding that Cdc42-regulates SC radial sorting (Benninger et al., 2007). Abnormally large axon bundles containing unsorted small, medium and large diameter axons were prevalent in Cdc42-CKO sciatic nerves. We analyzed adult mice and found that large unsorted bundles persist in adult Cdc42-CKO mice surrounded by SC nuclei, a morphology characteristic of developing peripheral nerves (Jessen and Mirsky, 2005; Martin and Webster, 1973; Webster et al., 1973). We also identified enlarged blood vessels in Cdc42-CKO nerves. Thin sciatic nerves in Cdc42-CKO mice could be rescued to near-normal size in Cdc42-CKO;NF2-del double mutants, with radial sorting also rescued. We also found that myelin was not maintained normally, in that abnormal infoldings and outfoldings of myelin sheath were observed in Cdc42-CKO myelinated axons, and that aberrant myelin sheath folding in Cdc42 mutants was NF2/merlin independent.

We relied on a NF2-del transgenic mouse to study merlin effects. The NF2-del transgenic and homozygous NF2 knockout mice (P0Cre; $Nf2^{flox2/flox2}$) have similar paranodal defects, SC hyperplasia, and develop tumors at comparable frequency between 9 and 20 months (Denisenko et al., 2008; Giovannini et al., 1999, 2000). Analysis of SC cultures from these two mouse strains reveals identical growth after confluence, and identical gene expression (Marco Giovannini, personal communication). Therefore NF2-del acts as dominant negative allele, enabling us to define merlin functions.

Axonal sorting defects in Cdc42-CKO nerves did not correlate with reduced numbers of available SCs. We did not observe significant differences in Ki67-positive cells at P0 Cdc42-CKO nerves compared with control nerves. In a previous study, loss of Cdc42 led to transiently reduced SC proliferation at late embryonic and perinatal stages (Benninger et al., 2007), and the authors postulated that appropriate proliferation during embryonic life, during radial sorting, was necessary for normal radial sorting. The difference between the studies may result from differences in mouse strain background and/or the Cdc42 knockout allele studied. At P30, SC proliferation and total nuclei number in Cdc42-CKO nerves was not affected by NF2/merlin mutation, although sorting was rescued. Several studies suggest that mammalian SC differentiation and proliferation can be differentially regulated events (Kim et al., 2000; Monje et al., 2010; Yang et al., 2008). For example, ErbB signaling was directly shown to play a role in radial sorting independent of SC number in zebrafish nerve (Raphael et al., 2011). Our study provides evidence to support the idea that SC sorting of axons is not directly coupled to SC proliferation.

We found that phosphorylation of FAK was reduced in Cdc42-CKO SCs. Reduced phosphorylation of FAK in Cdc42-CKO SCs was rescued by NF2/merlin mutation—which also rescued aberrant radial sorting. Our results are consistent with Cdc42 regulating FAK in other systems, and with the finding that knockout of FAK in SC causes sorting defects and myelin abnormalities very similar to those in Cdc42-CKO peripheral nerve (Grove et al., 2007; Yang et al., 2006; Zheng et al., 2009). Laminins bind integrin proteins that activate

FAK, which itself can bind a Cdc42-GAP, Graf (Hildebrand et al., 1996). It is therefore important that conditional loss of laminin γ-1 or β1-integrin in SCs also impair radial sorting (Chen and Strickland, 2003; Feltri et al., 2002). However, whether NF2/merlin plays a role in laminin-regulated SC sorting remains unclear given that we did not detect altered merlin phosphorylation in Cdc42-CKO nerves, even though laminin stimulates NF2/merlin phosphorylation in SC *in vitro* (Thaxton et al., 2008). Indeed, our finding that the radial sorting defect in Cdc42-CKO is rescued by merlin mutation implies that wild type merlin modulates SC radial sorting when Cdc42 is inactive.

A pathway in which laminins bind integrins to activate cdc42 and FAK may control axonal sorting, but the situation is likely to be more complex. Thus, similar to the Cdc42-CKO, in the β1-integrin knockout proliferation is not altered in the perinatal period (Feltri et al., 2002). In laminin γ-1 mutants only some Cre drivers reduce proliferation (Chen and Strickland, 2003; Yu et al., 2005), while loss of FAK reduced SC proliferation (Grove et al., 2007). In addition, Rac1 was implicated in sorting downstream of integrins (Nodari et al., 2007), and based on our findings Cdc42 and NF2/merlin also play roles. Consistent with our results, sorting defects in laminin mutants were improved by activation of Rac or Cdc42 (Yu et al., 2009).

Phosphorylation of GSK3β and expression of β-catenin were significantly decreased in Cdc42-CKO mice and were restored by mutation of NF2/merlin. WNT/β-catenin signaling normally regulates neural crest cell fate decisions and myelination in SCs, at least in some studies (Hari et al., 2012; Lewallen et al., 2011; Tawk et al., 2011). The β-catenin pathway stimulates remyelination (Makoukji et al., 2012), and it remains to be determined if Cdc42 plays a role in that setting. The NF2-del transgenic mice have numerous short internodes and decreased distances between Schmidt-Lanterman incisures (Denisenko et al., 2008). As our EM studies were entirely in cross-section, we did not evaluate Schmidt-Lanterman incisures. Intriguingly, active β-catenin is a component of Schmidt-Lanterman incisures (Tricaud et al., 2005), and it remains to be determined if Cdc42 plays a role in that phenotype. Cdc42 can control β-catenin stability through PKCζ-mediated phosphorylation of GSK3β(Wu et al., 2006), which may be relevant to our findings. Alternatively, Cdc42 can regulate this pathway through its effector PAR6 (Etienne-Manneville and Hall, 2003; Wu et al., 2006). In either case, FAK and β-catenin are candidate effectors of the NF2/merlin dependent function of Cdc42 in SC radial sorting that deserve additional study.

In normal cells, phosphorylation of NF2/merlin at serine 518 alters NF2/merlin conformation, enabling NF2/merlin interaction with specific binding partners (Rong et al., 2004; Ye, 2007). NF2/merlin phosphorylation can be mediated by PAK (Xiao et al., 2002; Yi et al., 2008). We previously reported that P-PAK (Thr423 (PAK1)/Thr402 (PAK2) and P-merlin (Ser518) are significantly decreased in Rac1-CKO SC, using the same DhhCre driver used in this study (Guo et al., 2012). In contrast, P-PAK and P-merlin were not altered in Cdc42-CKO sciatic nerves. Thus, PAK appears to be an effector of Rac1 but not Cdc42 in SCs *in vivo*, and NF2/merlin appears to play some roles in SC signaling independent of PAK. It remains possible that specific phosphorylated isoforms of PAK do change in the absence of Cdc42, as phosphorylation sites in PAK other than those we analyzed have been identified (Manser and Lim, 1999; Stockton et al., 2004).

Abnormal myelin including myelin infoldings and outfoldings with redundant myelin loops were frequently observed in Cdc42-CKO nerves. These imply a defect in myelin homeostasis, rather than myelin structure. Similar myelin abnormalities are observed in CMT disease, including mutation or loss of the myotubularin-related phosphatase MTMR (Previtali et al. 2007) and the Cdc42 GEF *FABIN/FGD4* (Delague et al., 2007; Stendel et al., 2007). Mouse models of *Mtmr2*, *Mtmr13* or *Frabin* disruption in mouse SCs show the myelin outfoldings (Bolino et al., 2004; Horn et al., 2012; Robinson et al., 2008; Tersar et al., 2007). Cdc42 activity was reduced in the absence of Fabin/FGD4, a Cdc42 GEF (Horn et al., 2012). This finding is consistent with our evidence that Cdc42 plays critical roles in regulating myelin folding and may be relevant to the CMT disease process. How loss of Cdc42 leads to SC pathological features in CMT disease remains unknown. Our results suggest that aberrant myelin sheath folding and *in vitro* SC process number and morphology in Cdc42 mutants are NF2/merlin independent. These phenotypes may be related to the well-studied role of Cdc42 in cell polarity, and might require Cdc42 effectors including IQGAP, WASP and/or PAR3/6 (Etienne-Manneville, 2004), but might also require Cdc42 effectors p38, JNK, or others still to be identified (Nakanishi and Takai, 2008).

Many collagen fibers ensheathed and wrapped by SCs were observed in Cdc42-CKO;NF2-del double mutant mice. Denisenko et al. (2008) identified similar, but fewer, collagen pockets in NF2-del mice and P0Cre; $NF2^{flox2/flox2}$ mice. SC process formation resulting in collagen fiber wrapping is likely to be regulated by NF2/merlin loss independent of Cdc42, perhaps through another small G protein activated by loss of Cdc42. SC-wrapped collagen fibers were also present in Pten-deficient SCs, which have elevated levels of phosphatidylinositol 3,4,5-trisphosphate (PIP3) (Goebbels et al., 2010). Considering that NF2/merlin can bind to PIP2 (Mani et al., 2011), PIP3 levels may be altered by NF2/merlin mutation and be relevant to this phenotype.

Overall, the ensheathment of small axons lost in Cdc42-CKO mice led to absence of mature Remak bundles. Additional loss of NF2/merlin function enabled ensheathment of small axons, but this ensheathment was exuberant, so that collagen was also wrapped. This finding is consistent with the idea that NF2/merlin normally feeds back to inhibit wrapping once each axon is wrapped, and supports the idea that merlin acts up and downstream of Cdc42.

Supplementary Material

Refer to Web version on PubMed Central for supplementary material.

Acknowledgments

NIH; Grant number: R01CA118032.

The authors thank Georgianne Ciraolo for assistance with electron microscopy, Dr. Marco Giovannini for providing NF2-delta2,3 (NF2-del) mice, and Dr. Robert Hennigan for helpful discussions.

References

Azzedine H, Bolino A, Taieb T, Birouk N, Di Duca M, Bouhouche A, Benamou S, Mrabet A, Hammadouche T, Chkili T, et al. Mutations in MTMR13, a new pseudophosphatase homologue of MTMR2 and Sbf1, in two families with an autosomal recessive demyelinating form of Charcot-

Marie-Tooth disease associated with early-onset glaucoma. Am J Hum Genet. 2003; 72:1141–1153. [PubMed: 12687498]

Benninger Y, Thurnherr T, Pereira JA, Krause S, Wu X, Chrostek-Grashoff A, Herzog D, Nave KA, Franklin RJ, Meijer D, et al. Essential and distinct roles for cdc42 and rac1 in the regulation of Schwann cell biology during peripheral nervous system development. J Cell Biol. 2007; 177:1051–1061. [PubMed: 17576798]

Bolino A, Bolis A, Previtali SC, Dina G, Bussini S, Dati G, Amadio S, Del Carro U, Mruk DD, Feltri ML, et al. Disruption of Mtmr2 produces CMT4B1-like neuropathy with myelin outfolding and impaired spermatogenesis. J Cell Biol. 2004; 167:711–721. [PubMed: 15557122]

Bolino A, Muglia M, Conforti FL, LeGuern E, Salih MAM, Georgiou DM, Christodoulou K, Hausmanowa-Petrusewicz I, Mandich P, Schenone A, et al. Charcot-Marie-Tooth type 4B is caused by mutations in the gene encoding myotubularin-related protein-2. Nat Genet. 2000; 25:17–19. [PubMed: 10802647]

Bos JL, Rehmann H, Wittinghofer A. GEFs and GAPs: Critical elements in the control of small G proteins. Cell. 2007; 129:865–877. [PubMed: 17540168]

Boyer O, Nevo F, Plaisier E, Funalot B, Gribouval O, Benoit G, Cong EH, Arrondel C, Tete MJ, Montjean R, et al. INF2 mutations in Charcot-Marie-Tooth disease with glomerulopathy. N Engl J Med. 2011; 365:2377–2388. [PubMed: 22187985]

Chen ZL, Strickland S. Laminin gamma1 is critical for Schwann cell differentiation, axon myelination, and regeneration in the peripheral nerve. J Cell Biol. 2003; 163:889–899. [PubMed: 14638863]

Chernousov MA, Yu WM, Chen ZL, Carey DJ, Strickland S. Regulation of Schwann cell function by the extracellular matrix. Glia. 2008; 56:1498–1507. [PubMed: 18803319]

Delague V, Jacquier A, Hamadouche T, Poitelon Y, Baudot C, Boccaccio I, Chouery E, Chaouch M, Kassouri N, Jabbour R, et al. Mutations in FGD4 encoding the Rho GDP/GTP exchange factor FRABIN cause autosomal recessive Charcot-Marie-Tooth type 4H. Am J Hum Genet. 2007; 81:1–16. [PubMed: 17564959]

Denisenko N, Cifuentes-Diaz C, Irinopoulou T, Carnaud M, Benoit E, Niwa-Kawakita M, Chareyre F, Giovannini M, Girault JA, Goutebroze L. Tumor suppressor schwannomin/merlin is critical for the organization of Schwann cell contacts in peripheral nerves. J Neurosci. 2008; 28:10472–10481. [PubMed: 18923024]

Etienne-Manneville S. Cdc42—The centre of polarity. J Cell Sci. 2004; 117(Part 8):1291–1300. [PubMed: 15020669]

Etienne-Manneville S, Hall A. Cdc42 regulates GSK-3beta and adenomatous polyposis coli to control cell polarity. Nature. 2003; 421:753–756. [PubMed: 12610628]

Evans DG, Huson SM, Donnai D, Neary W, Blair V, Newton V, Harris R. A clinical study of type 2 neurofibromatosis. Q J Med. 1992; 84:603–618. [PubMed: 1484939]

Fabrizi GM, Taioli F, Cavallaro T, Ferrari S, Bertolasi L, Casarotto M, Rizzuto N, Deconinck T, Timmerman V, De Jonghe P. Further evidence that mutations in FGD4/frabin cause Charcot-Marie-Tooth disease type 4H. Neurology. 2009; 72:1160–1164. [PubMed: 19332693]

Feltri ML, Graus Porta D, Previtali SC, Nodari A, Migliavacca B, Cassetti A, Littlewood-Evans A, Reichardt LF, Messing A, Quattrini A, et al. Conditional disruption of beta 1 integrin in Schwann cells impedes interactions with axons. J Cell Biol. 2002; 156:199–209. [PubMed: 11777940]

Flaiz C, Kaempchen K, Matthies C, Hanemann CO. Actin-rich protrusions and nonlocalized GTPase activation in Merlin-deficient schwannomas. J Neuropathol Exp Neurol. 2007; 66:608–616. [PubMed: 17620986]

Giovannini M, Robanus-Maandag E, Niwa-Kawakita M, van der Valk M, Woodruff JM, Goutebroze L, Merel P, Berns A, Thomas G. Schwann cell hyperplasia and tumors in transgenic mice expressing a naturally occurring mutant NF2 protein. Genes Dev. 1999; 13:978–986. [PubMed: 10215625]

Giovannini M, Robanus-Maandag E, van der Valk M, Niwa-Kawakita M, Abramowski V, Goutebroze L, Woodruff JM, Berns A, Thomas G. Conditional biallelic Nf2 mutation in the mouse promotes manifestations of human neurofibromatosis type 2. Genes Dev. 2000; 14:1617–1630. [PubMed: 10887156]

Goebbels S, Oltrogge JH, Kemper R, Heilmann I, Bormuth I, Wolfer S, Wichert SP, Mobius W, Liu X, Lappe-Siefke C, et al. Elevated phosphatidylinositol 3,4,5-trisphosphate in glia triggers cell-autonomous membrane wrapping and myelination. J Neurosci. 2010; 30:8953–8964. [PubMed: 20592216]

Grove M, Komiyama NH, Nave KA, Grant SG, Sherman DL, Brophy PJ. FAK is required for axonal sorting by Schwann cells. J Cell Biol. 2007; 176:277–282. [PubMed: 17242067]

Guo L, Moon C, Niehaus K, Zheng Y, Ratner N. Rac1 controls Schwann cell myelination through cAMP and NF2/merlin. J Neurosci. 2012; 32:17251–17261. [PubMed: 23197717]

Hari L, Miescher I, Shakhova O, Suter U, Chin L, Taketo M, Richardson WD, Kessaris N, Sommer L. Temporal control of neural crest lineage generation by Wnt/beta-catenin signaling. Development. 2012; 139:2107–2117. [PubMed: 22573620]

Hildebrand JD, Taylor JM, Parsons JT. An SH3 domain-containing GTPase-activating protein for Rho and Cdc42 associates with focal adhesion kinase. Mol Cell Biol. 1996; 16:3169–3178. [PubMed: 8649427]

Horn M, Baumann R, Pereira JA, Sidiropoulos PN, Somandin C, Welzl H, Stendel C, Luhmann T, Wessig C, Toyka KV, et al. Myelin is dependent on the Charcot-Marie-Tooth Type 4H disease culprit protein FRABIN/FGD4 in Schwann cells. Brain. 2012; 135(Part 12):3567–3583. [PubMed: 23171661]

Jaegle M, Ghazvini M, Mandemakers W, Piirsoo M, Driegen S, Levavasseur F, Raghoenath S, Grosveld F, Meijer D. The POU proteins Brn-2 and Oct-6 share important functions in Schwann cell development. Genes Dev. 2003; 17:1380–1391. [PubMed: 12782656]

Jessen KR, Mirsky R. The origin and development of glial cells in peripheral nerves. Nat Rev Neurosci. 2005; 6:671–682. [PubMed: 16136171]

Jin F, Dong B, Georgiou J, Jiang Q, Zhang J, Bharioke A, Qiu F, Lommel S, Feltri ML, Wrabetz L, et al. N-WASp is required for Schwann cell cytoskeletal dynamics, normal myelin gene expression and peripheral nerve myelination. Development. 2011; 138:1329–1337. [PubMed: 21385763]

Kim HA, Pomeroy SL, Whoriskey W, Pawlitzky I, Benowitz LI, Sicinski P, Stiles CD, Roberts TM. A developmentally regulated switch directs regenerative growth of Schwann cells through cyclin D1. Neuron. 2000; 26:405–416. [PubMed: 10839359]

Lewallen KA, Shen YA, De la Torre AR, Ng BK, Meijer D, Chan JR. Assessing the role of the cadherin/catenin complex at the Schwann cell-axon interface and in the initiation of myelination. J Neurosci. 2011; 31:3032–3043. [PubMed: 21414924]

Makoukji J, Belle M, Meffre D, Stassart R, Grenier J, Shackleford G, Fledrich R, Fonte C, Branchu J, Goulard M, et al. Lithium enhances remyelination of peripheral nerves. Proc Natl Acad Sci USA. 2012; 109:3973–3978. [PubMed: 22355115]

Mani T, Hennigan RF, Foster LA, Conrady DG, Herr AB, Ip W. FERM domain phosphoinositide binding targets merlin to the membrane and is essential for its growth-suppressive function. Mol Cell Biol. 2011; 31:1983–1996. [PubMed: 21402777]

Manser E, Lim L. Roles of PAK family kinases. Prog Mol Subcell Biol. 1999; 22:115–133. [PubMed: 10081067]

Martin JR, Webster HD. Mitotic Schwann cells in developing nerve: Their changes in shape, fine structure, and axon relationships. Dev Biol. 1973; 32:417–431. [PubMed: 4789699]

Monje PV, Soto J, Bacallao K, Wood PM. Schwann cell dedifferentiation is independent of mitogenic signaling and uncoupled to proliferation: Role of cAMP and JNK in the maintenance of the differentiated state. J Biol Chem. 2010; 285:31024–31036. [PubMed: 20634285]

Nakanishi H, Takai Y. Frabin and other related Cdc42-specific guanine nucleotide exchange factors couple the actin cytoskeleton with the plasma membrane. J Cell Mol Med. 2008; 12:1169–1176. [PubMed: 18410521]

Nodari A, Zambroni D, Quattrini A, Court FA, D'Urso A, Recchia A, Tybulewicz VL, Wrabetz L, Feltri ML. Beta1 integrin activates Rac1 in Schwann cells to generate radial lamellae during axonal sorting and myelination. J Cell Biol. 2007; 177:1063–1075. [PubMed: 17576799]

Previtali SC, Quattrini A, Bolino A. Charcot-Marie-Tooth type 4B demyelinating neuropathy: deciphering the role of MTMR phosphatases. Expert Rev Mol Med. 2007; 9:1–16. [PubMed: 17880751]

Raphael AR, Lyons DA, Talbot WS. ErbB signaling has a role in radial sorting independent of Schwann cell number. Glia. 2011; 59:1047–1055. [PubMed: 21491500]

Robinson FL, Niesman IR, Beiswenger KK, Dixon JE. Loss of the inactive myotubularin-related phosphatase Mtmr13 leads to a Charcot-Marie-Tooth 4B2-like peripheral neuropathy in mice. Proc Natl Acad Sci USA. 2008; 105:4916–4921. [PubMed: 18349142]

Rong R, Surace EI, Haipek CA, Gutmann DH, Ye K. Serine 518 phosphorylation modulates merlin intramolecular association and binding to critical effectors important for NF2 growth suppression. Oncogene. 2004; 23:8447–8454. [PubMed: 15378014]

Stendel C, Roos A, Deconinck T, Pereira J, Castagner F, Niemann A, Kirschner J, Korinthenberg R, Ketelsen UP, Battaloglu E, et al. Peripheral nerve demyelination caused by a mutant Rho GTPase guanine nucleotide exchange factor, frabin/FGD4. Am J Hum Genet. 2007; 81:158–164. [PubMed: 17564972]

Stockton RA, Schaefer E, Schwartz MA. p21-activated kinase regulates endothelial permeability through modulation of contractility. J Biol Chem. 2004; 279:46621–46630. [PubMed: 15333633]

Tawk M, Makoukji J, Belle M, Fonte C, Trousson A, Hawkins T, Li H, Ghandour S, Schumacher M, Massaad C. Wnt/beta-catenin signaling is an essential and direct driver of myelin gene expression and myelinogenesis. J Neurosci. 2011; 31:3729–3742. [PubMed: 21389228]

Tersar K, Boentert M, Berger P, Bonneick S, Wessig C, Toyka KV, Young P, Suter U. Mtmr13/Sbf2-deficient mice: An animal model for CMT4B2. Hum Mol Genet. 2007; 16:2991–3001. [PubMed: 17855448]

Thaxton C, Lopera J, Bott M, Baldwin ME, Kalidas P, Fernandez-Valle C. Phosphorylation of the NF2 tumor suppressor in Schwann cells is mediated by Cdc42-Pak and requires paxillin binding. Mol Cell Neurosci. 2007; 34:231–242. [PubMed: 17175165]

Thaxton C, Lopera J, Bott M, Fernandez-Valle C. Neuregulin and laminin stimulate phosphorylation of the NF2 tumor suppressor in Schwann cells by distinct protein kinase A and p21-activated kinase-dependent pathways. Oncogene. 2008; 27:2705–2715. [PubMed: 17998937]

Tricaud N, Perrin-Tricaud C, Bruses JL, Rutishauser U. Adherens junctions in myelinating Schwann cells stabilize Schmidt-Lanterman incisures via recruitment of p120 catenin to E-cadherin. J Neurosci. 2005; 25:3259–3269. [PubMed: 15800180]

Webster HD, Martin R, O'Connell MF. The relationships between interphase Schwann cells and axons before myelination: A quantitative electron microscopic study. Dev Biol. 1973; 32:401–416. [PubMed: 4789698]

Wu J, Williams JP, Rizvi TA, Kordich JJ, Witte D, Meijer D, Stemmer-Rachamimov AO, Cancelas JA, Ratner N. Plexiform and dermal neurofibromas and pigmentation are caused by Nf1 loss in desert hedgehog-expressing cells. Cancer Cell. 2008; 13:105–116. [PubMed: 18242511]

Wu X, Quondamatteo F, Lefever T, Czuchra A, Meyer H, Chrostek A, Paus R, Langbein L, Brakebusch C. Cdc42 controls progenitor cell differentiation and beta-catenin turnover in skin. Genes Dev. 2006; 20:571–585. [PubMed: 16510873]

Xiao GH, Beeser A, Chernoff J, Testa JR. p21-activated kinase links Rac/Cdc42 signaling to merlin. J Biol Chem. 2002; 277:883–886. [PubMed: 11719502]

Yamauchi J, Chan JR, Miyamoto Y, Tsujimoto G, Shooter EM. The neurotrophin-3 receptor TrkC directly phosphorylates and activates the nucleotide exchange factor Dbs to enhance Schwann cell migration. Proc Natl Acad Sci USA. 2005; 102:5198–5203. [PubMed: 15758069]

Yang DP, Zhang DP, Mak KS, Bonder DE, Pomeroy SL, Kim HA. Schwann cell proliferation during Wallerian degeneration is not necessary for regeneration and remyelination of the peripheral nerves: Axon-dependent removal of newly generated Schwann cells by apoptosis. Mol Cell Neurosci. 2008; 38:80–88. [PubMed: 18374600]

Yang L, Wang L, Zheng Y. Gene targeting of Cdc42 and Cdc42GAP affirms the critical involvement of Cdc42 in filopodia induction, directed migration, and proliferation in primary mouse embryonic fibroblasts. Mol Biol Cell. 2006; 17:4675–4685. [PubMed: 16914516]

Ye K. Phosphorylation of merlin regulates its stability and tumor suppressive activity. Cell Adh Migr. 2007; 1:196–198. [PubMed: 19262146]

Yi C, Wilker EW, Yaffe MB, Stemmer-Rachamimov A, Kissil JL. Validation of the p21-activated kinases as targets for inhibition in neurofibromatosis type 2. Cancer Res. 2008; 68:7932–7937. [PubMed: 18829550]

Yu WM, Chen ZL, North AJ, Strickland S. Laminin is required for Schwann cell morphogenesis. J Cell Sci. 2009; 122(Part 7):929–936. [PubMed: 19295124]

Yu WM, Feltri ML, Wrabetz L, Strickland S, Chen ZL. Schwann cell-specific ablation of laminin gamma 1 causes apoptosis and prevents proliferation. J Neurosci. 2005; 25:4463–4472. [PubMed: 15872093]

Zhan Y, Chadee DN. Inhibition of Cdc42-mediated activation of mixed lineage kinase 3 by the tumor suppressor protein merlin. Small GTPases. 2010; 1:183–186. [PubMed: 21686274]

Zheng Y, Xia Y, Hawke D, Halle M, Tremblay ML, Gao X, Zhou XZ, Aldape K, Cobb MH, Xie K, et al. FAK phosphorylation by ERK primes ras-induced tyrosine dephosphorylation of FAK mediated by PIN1 and PTP-PEST. Mol Cell. 2009; 35:11–25. [PubMed: 19595712]

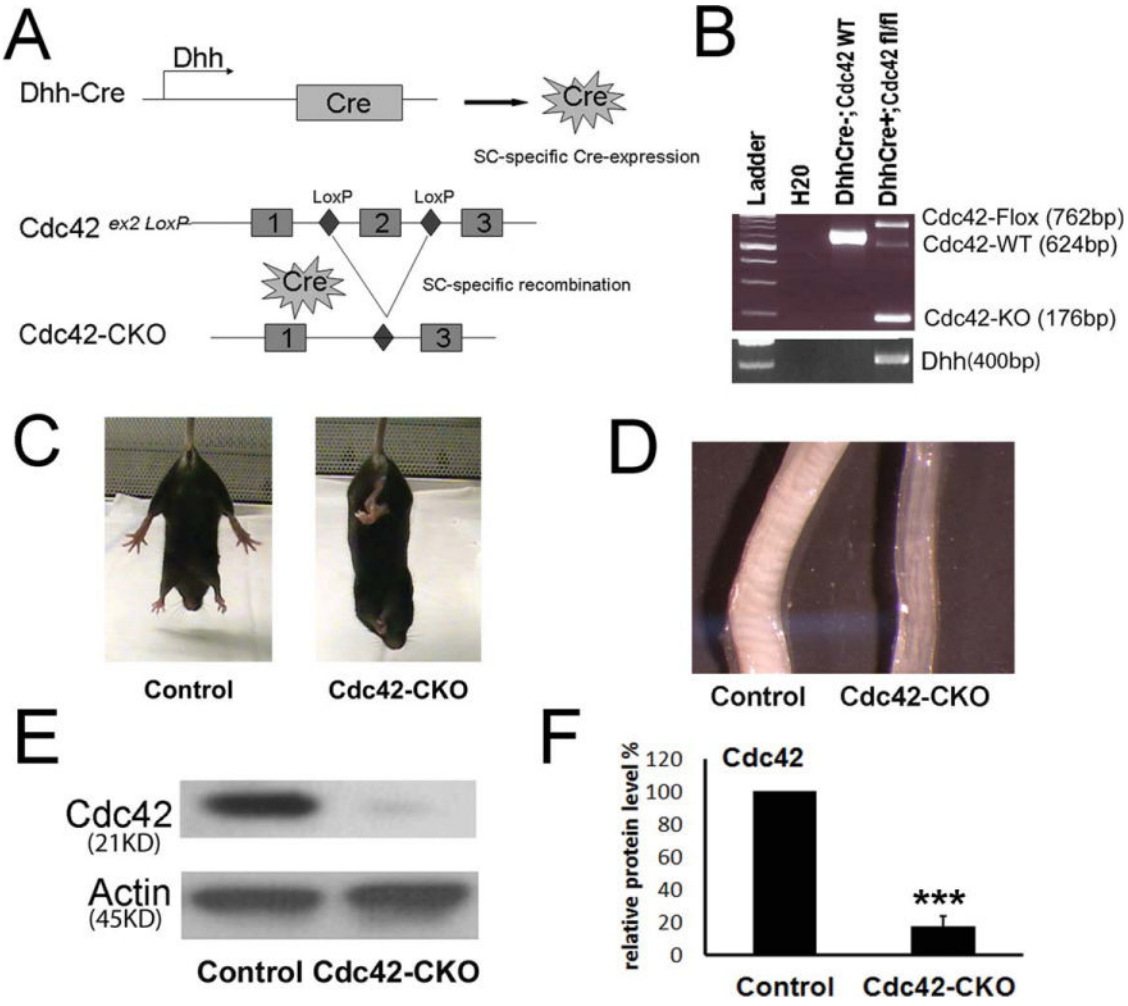

FIGURE 1.

Generation of Cdc42 conditional knockout mice. (**A**) Dhh-Cre directed recombination in Cdc42 mutant mice. Dhh activates Cre recombinase expression in SC from E12.5. Upon Cre recombination, exon 2 of the Cdc42 alleles between loxP sites is excised. (**B**) Genotyping for Dhh, *Cdc42* wild-type (WT), floxed (fl) and deletion (KO) alleles in control (*DhhCre−; Cdc42*$^{flox/WT}$) and Cdc42-CKO (*DhhCre+; Cdc42*$^{flox/flox}$) mice tails. (**C**) Control and Cdc42-CKO P30 mice are shown. Hind limb dysfunction in Cdc42-CKO mice was present and as noted by retracting hind limbs in photo. (**D**) Sciatic nerves from P30 Cdc42-CKO and control mice are shown. Cdc42-CKO sciatic nerves are thinner than control nerves. (**E**) Western blot analysis shows Cdc42 protein levels are decreased in P30 sciatic nerves of mutant mice. (**F**) Cdc42 protein levels are significantly decreased in scans of western blots from control and Cdc42-CKO nerves ($n = 4$). ***$P < 0.001$ by t test. Error bars indicate ± SEM.

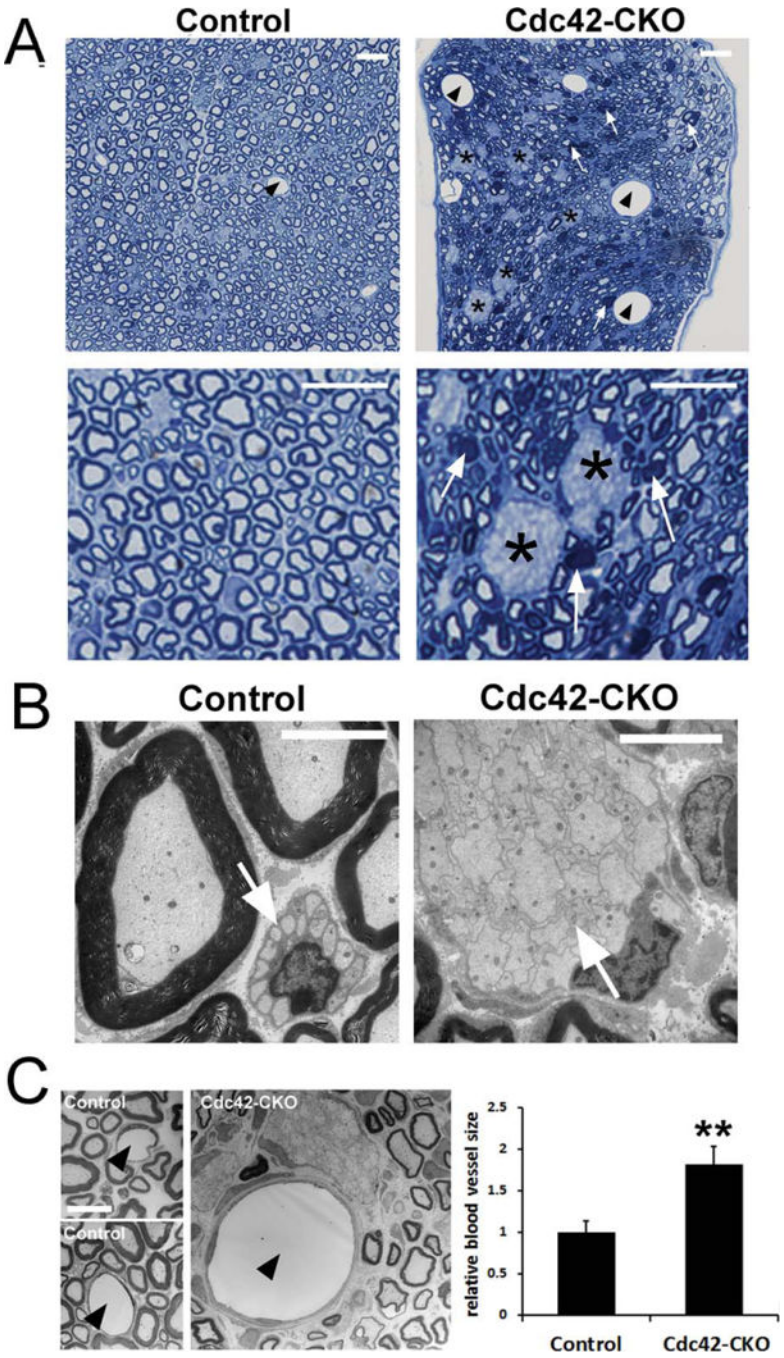

FIGURE 2.

Abnormal sciatic nerve structure in Cdc42-CKO mice. (**A**) Semi-thin cross-sections of adult control and Cdc42-CKO sciatic nerves. Large axonal bundles remained in Cdc42-CKO sciatic nerves (black asterisks). Some abnormal myelin sheath structure was observed in Cdc42-CKO sciatic nerves (white arrows). Enlarged blood vessels exist in Cdc42-CKO sciatic nerves (black arrowheads). (**B**) Electron microscopy (EM) shows normal Remak bundle in control nerve and large unsorted axon bundles with small and medium sized axons in Cdc42-CKO sciatic nerves. (**C**) EM shows blood vessel lumen (arrowheads) in control

and Cdc42-CKO nerves, with endothelial cell nuclei and processes surrounding nerve capillaries. Blood vessel size was increased in Cdc42-CKO mice (n = 4). Bars: (**A**) 10 μM; (**B**) 5 μM; (**C**) 10 μM.

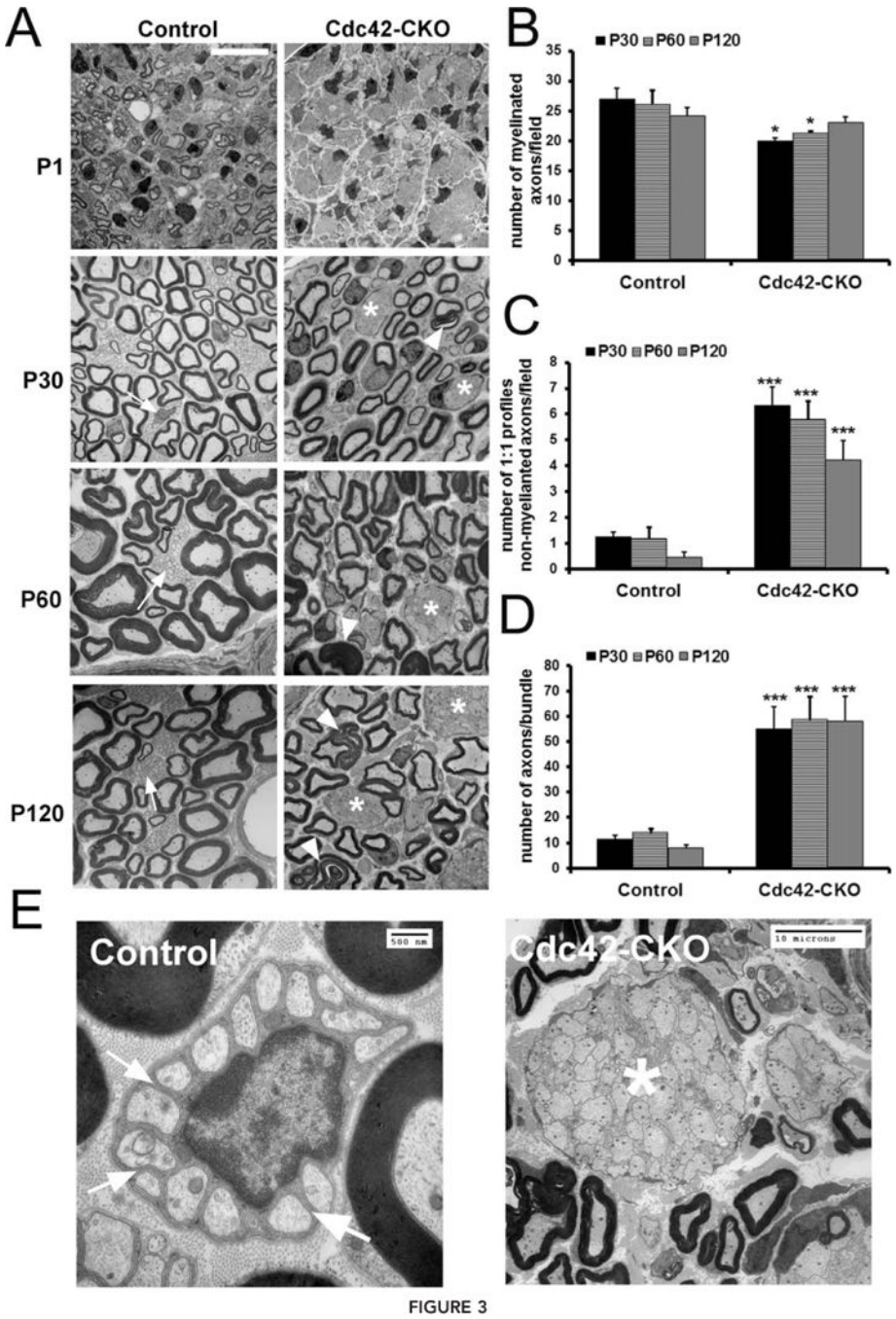

FIGURE 3

FIGURE 3.

Radial sorting defect in Cdc42-CKO mice. (**A**) EM shows that at P1, SCs were largely sorted and formed a few myelin sheaths in control sciatic nerves. In contrast, large axonal bundles were present and no myelin sheaths were detected in Cdc42-CKO sciatic nerves. At P30, P60 and P120, SCs had formed myelin sheaths around large axons (myelinating SCs) and Remak bundles (arrows) containing small axons (non-myelinating SCs) had formed in control nerves. However, large unsorted axon bundles (asterisks) with small and medium sized axons were found in Cdc42-CKO sciatic nerves. Abnomal folding of myelin sheaths

(arrowheads) also existed in Cdc42-CKO SC myelinating large axons. (**B**) There was no significant change in number of myelinated axons in Cdc42-CKO nerves compared to control nerves. (**C**) The number of unmyelinated SCs in 1:1 SC-axon profiles was increased in Cdc42-CKO nerves compared to control nerves. (**D**) There was a significant increase of axonal bundle size (axons/bundle) in Cdc42-CKO sciatic nerves. For (B–D), $n \geq 25$ fields from at least five animals per genotype. $^{*}P < 0.05$, $^{**}P < 0.01$, $^{***}P < 0.001$ by ANOVA followed by Tukey test. (**E**) While normal mature Remak bundles containing small axons individually ensheathed by membrane-delimited SC cytoplasm processes (arrow), in Cdc42-CKO mice axons touched each other with no intervening SC processes (asterisk) Error bars indicate ± SEM. Bar: (**A**) 10 μM.

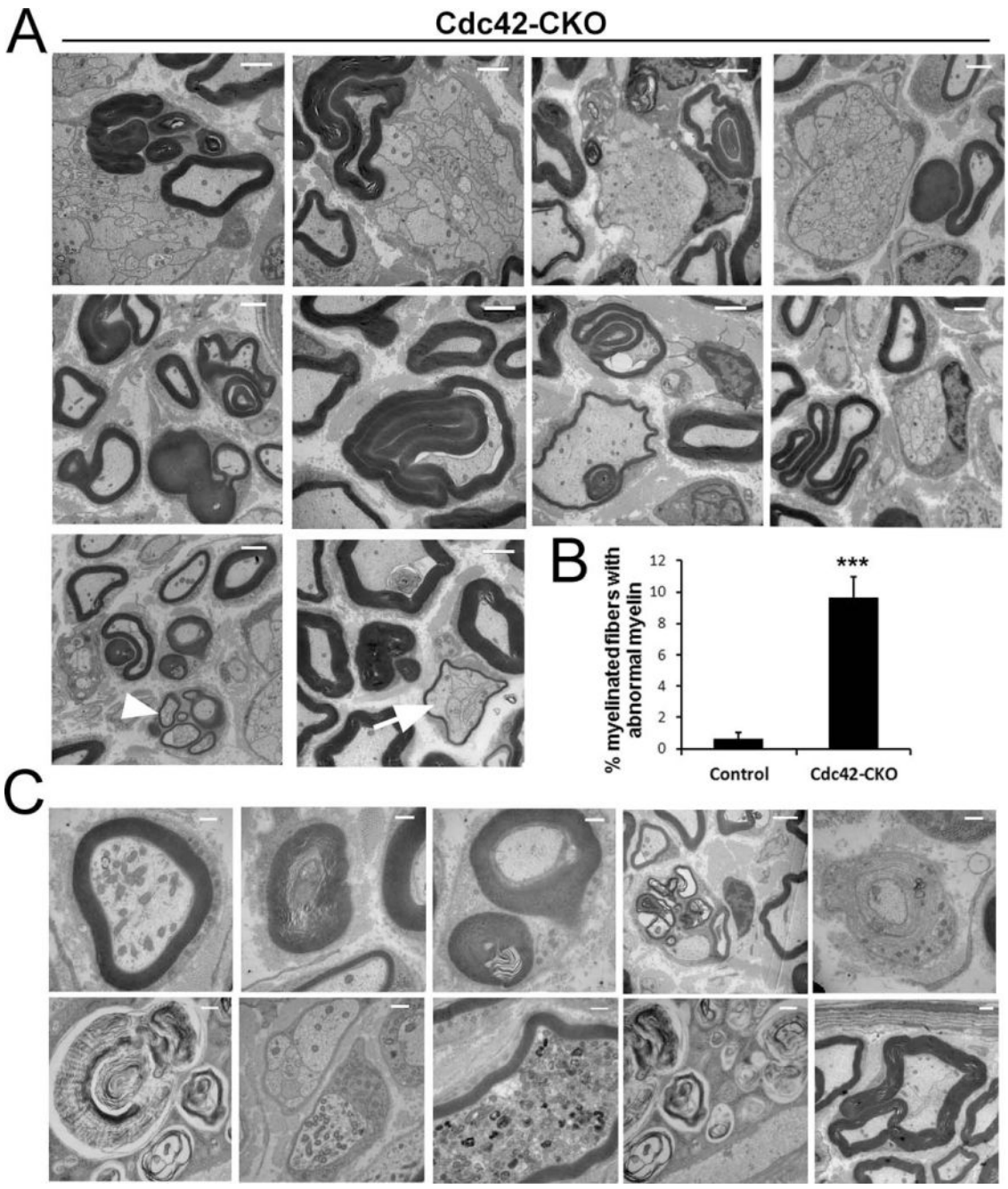

FIGURE 4.

Aberrant myelin morphology in Cdc42-CKO sciatic nerves. (**A**) EM of Cdc42-CKO sciatic nerves showed dysmyelination phenotypes. Cdc42-CKO nerve fibers showed abnormal features including myelin infoldings and outfoldings with redundant myelin loops. Bundles of small regenerating axons were present as groups of thinly myelinated axons (arrowhead). Occasionally, myelin sheaths wrapped around unsorted axons (arrow). (**B**) The number of abnormal myelin fibers was significantly increased in Cdc42-CKO nerves (n = 25 fields from five animals). ***P < 0.001 by t test. Error bars indicate 6 SEM. (**C**) Axonal

degeneration in Cdc42-CKO nerves, with accumulation of axonal organelles and myelin debris. Bars: (**A**) 2 μM; (**C**) 1 μM.

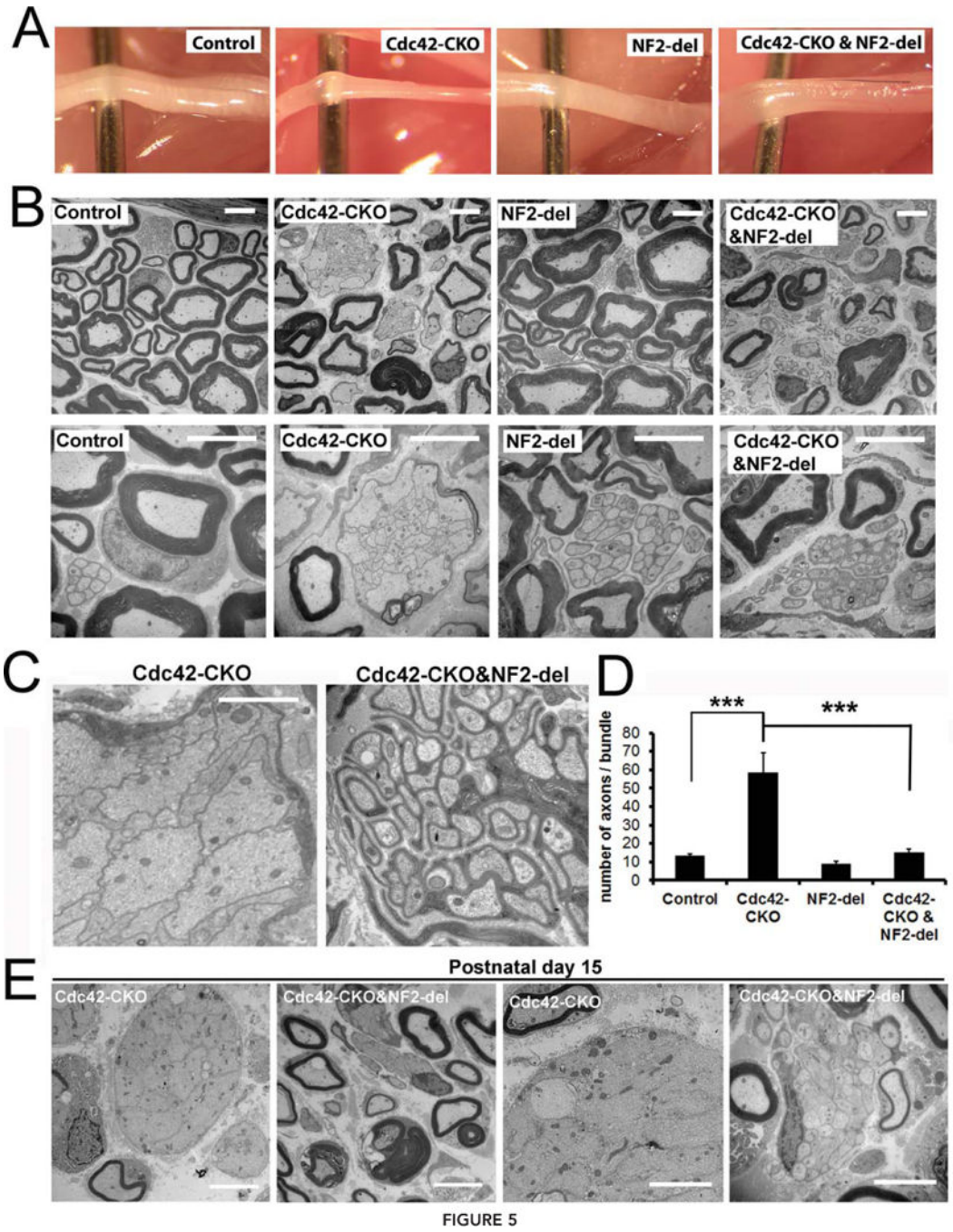

FIGURE 5

FIGURE 5.

Axonal sorting defects in Cdc42-CKO mice are rescued by NF2-del expression. (**A**) Sciatic nerves from 2-month-old control, Cdc42-CKO, NF2-del and Cdc42-CKO;NF2-del mice are shown. Cdc42-CKO sciatic nerve was thinner than control nerve, but nerve in Cdc42-CKO;NF2-del double mutant mice has a similar size to control nerve. (**B**) EM analysis of sciatic nerve cross-sections from control, Cdc42-CKO, NF2-del and Cdc42-CKO;NF2-del littermates at P60. Most of the large unsorted axons in Cdc42-CKO were sorted by SCs process in Cdc42-CKO;NF2-del double mutant mice. (**C**) High magnification images show

unmyelinating axon bundles in Cdc42-CKO mice and Cdc42-CKO;NF2-del double mutant mice. Unsegregated large and small axons were present in axon bundles in Cdc42-CKO mice. Individual small axons were segregated by SCs in Cdc42-CKO;NF2-del double mutant mice. (**D**) There is a significant decrease in number of axons ensheathed by single SC in Cdc42-CKO;NF2-del mice versus Cdc42-CKO mice (n = 6 animals/genotype). *P < 0.05, **P < 0.01, ***P < 0.001 by ANOVA followed by Tukey test. Error bars indicate ± SEM. (**E**) EM analysis of sciatic nerve cross-sections in Cdc42-CKO and Cdc42-CKO;NF2-del nerves at P15. Large bundles contain large axons in CDC42-CKO nerves at P15. In the Cdc42-CKO;NF2-del double mutants, bundles of unmyelinated axons contained mainly small axons, and larger axons were often present at the edges of bundles; some large fibers were thinly myelinated. Bars: (**B**) and (**E**) 5 μm; (**C**) 2 μm.

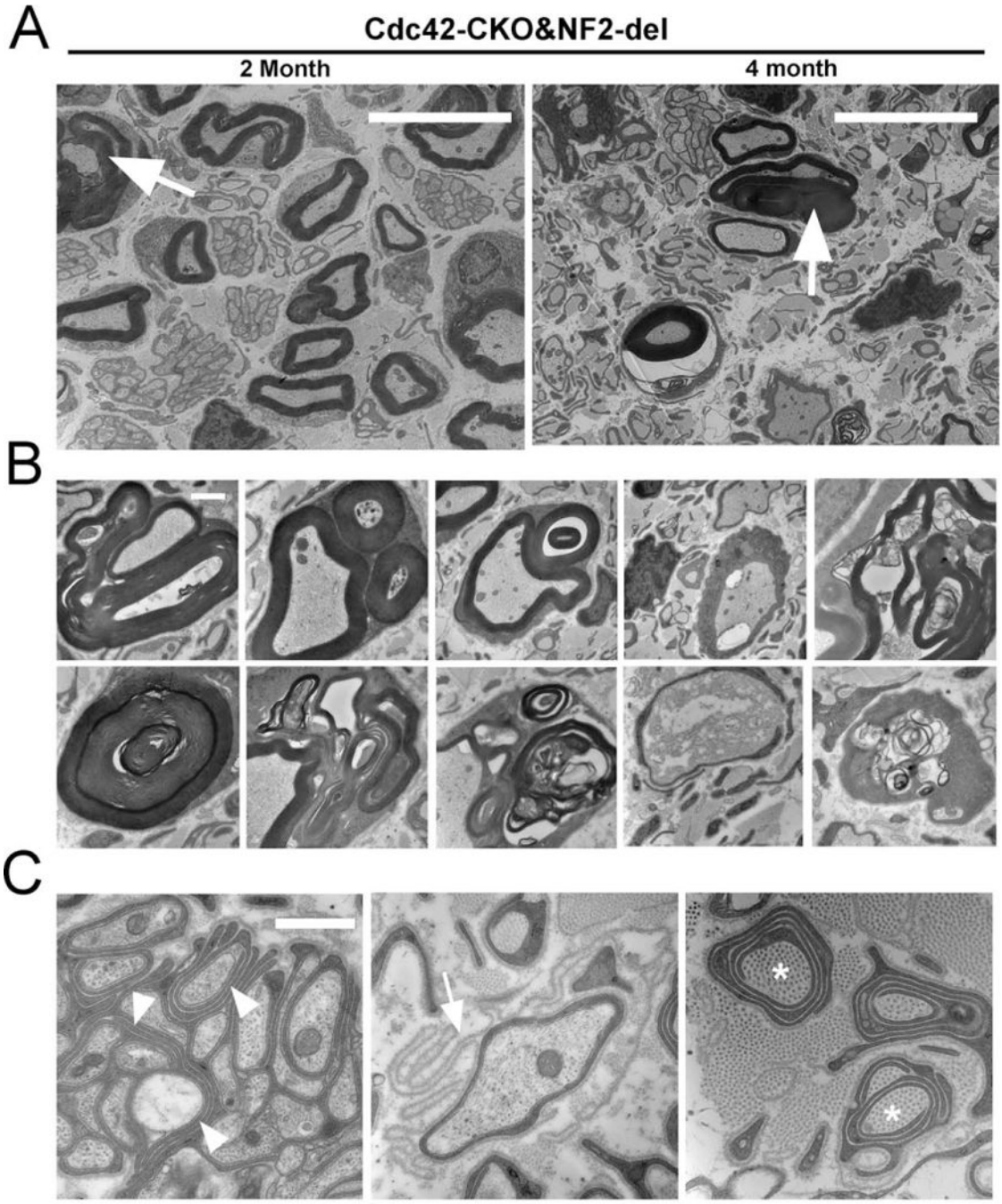

FIGURE 6.

Myelin abnormalities in Cdc42-CKO;NF2-del double mutant mice. (**A**) Electron micrographs of sciatic nerve sections in 2-and 4-month-old Cdc42-CKO;NF2-del double mutant mice. Abnormal folding of myelin sheath (arrows) was persistent in Cdc42-CKO;NF2-del nerves. (**B**) Myelin infoldings and outfoldings were persisted in Cdc42-CKO;NF2-del double mutant nerves. Axon degeneration was also observed. (**C**) Redundant SC process within axonal bundles (arrowheads), empty basal lamina loops (arrow), collagen

pockets (asterisks) (which are collagen surrounded by SC processes), and SC processes without axon contact were present. Bars: (**A**) 10 μm, (**B**) and (**C**) 1 μm.

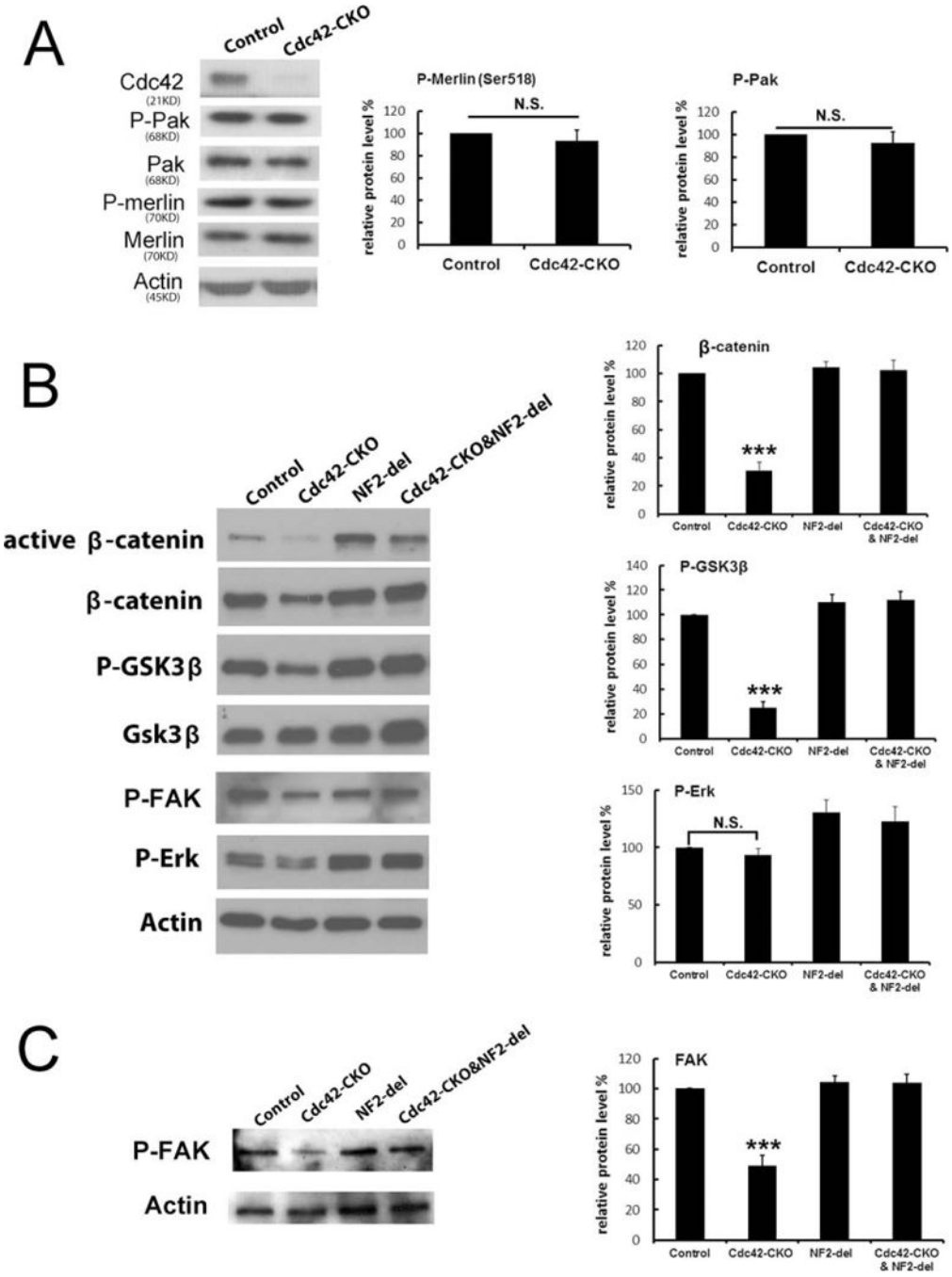

FIGURE 7.

Altered phosphorylation of FAK and GSK3*β*- *β*-catenin signaling is restored by mutation of NF2/merlin. (**A**) Phosphorylation of Pak (P-Pak_Thr423, Thr402) and merlin (P-merlin_S518) was not changed in Cdc42-CKO sciatic nerves. Actin expression was used as a protein loading control. (**B**) Phosphorylation of GSK3*β*, the expression of *β*-catenin and P-FAK were decreased in Cdc42-CKO mice and restored by mutation of NF2/merlin. (**C**) Reduced phosphorylation of FAK in lysates from cultured Cdc42-CKO SCs was also rescued by NF2/merlin mutation in Cdc42-CKO;NF2-del SCs. Blots are representative of at

least four independent experiments for each genotype. *$P < 0.05$, **$P < 0.01$, ***$P < 0.001$ by ANOVA followed by Tukey test. Error bars indicate ± SEM.

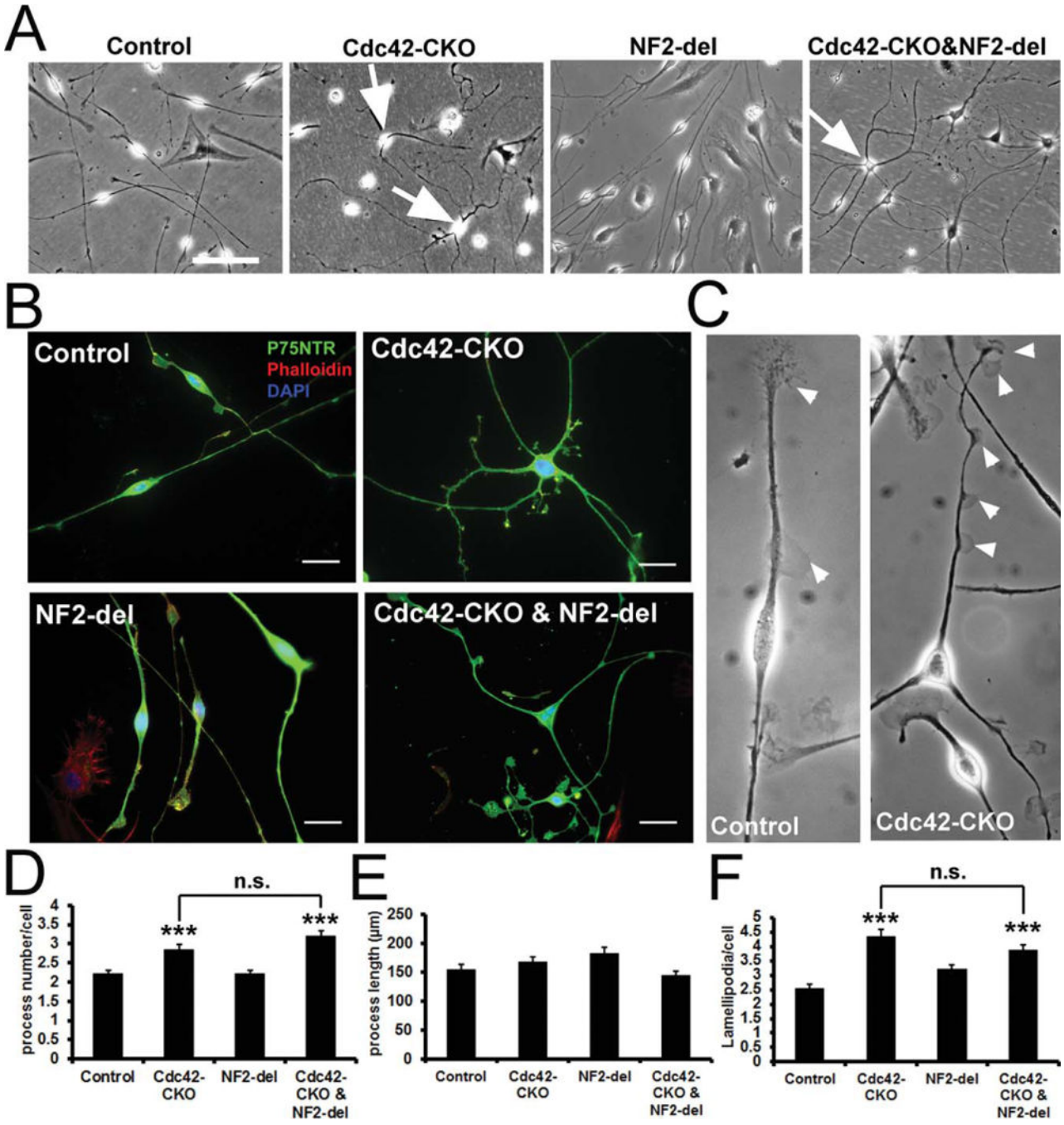

FIGURE 8.

Altered SC morphology in Cdc42-CKO SC culture is not affected by NF2-del expression. (**A**) SC cultures from control, Cdc42-CKO, NF2-del and Cdc42-CKO;NF2-del sciatic nerves are shown. Some SCs in Cdc42-CKO and Cdc42-CKO;NF2-del culture have multiple processes (arrows) rather than bipolar SC morphology in control culture. (**B**) Cultured SCs were immunostained with P75NTR (a SC specific marker, green) and Phalloidin (F-actin cytoskeleton, red). Nuclei were visualized by DAPI (blue). (**C**) Lamellipodia (arrowheads) in control and Cdc42-CKO SCs culture. (**D**) SC process number

per cell was increased in Cdc42-CKO. The increased SC process number in the absence of Cdc42 was not significantly affected by NF2/merlin in Cdc42-CKO;NF2-del cultures. (**E**) The average SC process length was not significantly changed by Cdc42-CKO or NF2/merlin mutant. (**F**) Lamellipodia per cell was increased in Cdc42-CKO SCs. The increased Lamellipodia numbers in the absence of Cdc42 was not significantly affected by NF2/merlin in Cdc42-CKO;NF2-del cultures. For (**C**), (**D**), and (**E**), $n \geq 50$ cells from three independent experiments per genotype. *$P < 0.05$, **$P < 0.01$, ***$P < 0.001$ by ANOVA followed by Tukey post hoc test. Error bars indicate ± SEM. Bars: (**A**) 100 μm; (**B**) 25 μm.